This article has been accepted for publication in a future issue of this journal, but has not been fully edited. Content may change prior to final publication. Citation information: DOI 10.1109/LAWP.2016.2585127, IEEE Antennas and Wireless Propagation Letters

Mutual Coupling Reduction in Dielectric Resonator Antennas Using Metasurface Shield for 60 GHz MIMO Systems

Abdolmehdi Dadgarpour, *Member IEEE*, Behnam Zarghooni, Bal S.Virdee, Tayeb A. Denidni, *Senior member, IEEE* and Ahmed A. Kishk, *Fellow, IEEE*

***Abstract*—An effective technique for reducing the mutual coupling between two Dielectric Resonator Antennas (DRA) operating at 60 GHz bands is presented. This is achieved by incorporating a metasurface between the two DRAs, which are arranged in the H-plane. The metasurface comprises an array of unique split-ring resonator (SRR) cells that are integrated along the E-plane. The SRR configuration is designed to provide band-stop functionality within the antenna bandwidth. By loading the DRA with 1×7 array of SRR unit cells, a 28 dB reduction in the mutual coupling level is achieved without compromising the antenna performance. The measured isolation of the prototype antenna varies from -30 to -46.5 dB over 59.3–64.8 GHz. The corresponding reflection coefficient of the DRA is better than -10 dB over 56.6–64.8 GHz.**

***Index Terms*—Dielectric resonator antenna, MIMO, millimeter-wave antenna, split-ring resonator, mutual coupling**

I. Introduction

MULTIGIGABIT wireless networks are on the cusp of economic viability with the worldwide availability of the unlicensed spectrum at 60 GHz. Also, recent advances in the millimeter-wave RF integrated circuits and devices in low cost encouraged their use. This is evident by the significant industry interest in this technology for various indoor applications such as wireless personal area networks [1], wireless local area networks [2], and wireless uncompressed HDTV [3]. The use of the 60 GHz band is also becoming very attractive for outdoor mesh networks with relatively short links of 100–200 m, in particular for the emerging 5G wireless cellular networks and Internet-of-Things (IoT). However, oxygen absorption in the 60 GHz band produces propagation losses of 10–16 dB/km, which adds about 3 dB to the link budget for a 200 m link. Such multi-gigabit outdoor mesh networks will provide an easily deployable broadband infrastructure that can have a multitude of applications, including wireless backhaul for Pico cellular networks as an alternative of the fiber optics for the users.

With the availability of several gigahertz of the unlicensed spectrum, this millimeter-wave technology should enable the substantial growth of data traffic with the advent of IoT. In order to accommodate the ever growing high capacity expected demand in the near future, the need for Multiple-input Multiple-output (MIMO) antennas that can provide spatial multiplexing gain, diversity gain, and interference reduction capability is evident. To improve the spectral efficiency of wireless systems using MIMO requires low correlation and high isolation between antennas.

A. Dadgarpour, and. A.A.Kishk are with Electrical and Computer Engineering department of Concordia university, Montreal, QC, H3G 1M8, CANADA (Email: mehdidadgar60@gmail.com), T.A. Denidni is with INRS-EMT, Montreal, QC, CANADA. B.Zarghooni is with Poly-Grames research center, École Polytechnique de Montréal. B.S. Virdee is with the Center for Communications Technology at London Metropolitan University, UK.

This requires low mutual coupling between the elements. It is reported in [20-22] that the dielectric resonator antenna (DRA) provides lower mutual coupling levels. However, further mutual coupling reduction is required.In this effort, a great deal of work has been reported to date on reducing the mutual coupling between antennas including application of (i) parasitic elements [4] [5], (ii) EBG structures [6] -[12], and (iii) metamaterial-based resonators [13] -[16]. Recently, the authors in [17] have introduced a double-layer mushroom EBG wall loaded between four cavities-backed slot antennas to reduce the mutual coupling between the antennas by 16 dB at 2.4 GHz. However, this structure is large and by adding the EBG wall, the antenna height is increased considerably. Another approach to reducing the effect of mutual coupling is reported in [18] involves integrating split-ring resonators in the ground plane of the patch antenna. This technique is shown to provide isolation improvement by 10 dB. However, the gain radiation pattern is not appropriate. Another technique in [19] uses parasitic elements to reduce the mutual coupling between antennas by 6 dB at 2.4 GHz. In [20], a new EBG structure loading between two DRA antennas is used to suppress the surface waves, and the coupling is reduced by 13 dB over 57-64 GHz. This approach, however, is only applicable to the arrangement of the antenna in the E-plane.

In this paper, an effective technique is demonstrated to improve substantially the isolation between two adjacent DRAs operating at 60 GHz for MIMO application. This is achieved by using a metasurface shield constructed of a unique split-ring resonator that is designed to provide band-stop functionality over the operating frequency range centered at 60 GHz. By integrating the array of SRR cell structure between the H-plane DRs along the E-plane results in a substantial reduction in the mutual coupling between the adjacent radiators. Using the proposed technique the isolation between the antennas is measured to be -46.5 dB at 60.4 GHz, which is an improvement by 31.5 dB. The isolation achieved with this technique is substantially better than techniques reported to date. The latest technique reported in [17] provides an isolation enhancement of only 16 dB.

II. Split-Ring Resonator Unit cell

This section presents the characteristic properties of a metasurface shield employed in the proposed DRA. The metasurface comprises a unique metamaterial unit cell, shown in Fig. 1, which is constructed from a split-ring resonator where the conductive elements create the inductance and the gap in the ring creates capacitance. Loading within the split-ring structure is a smaller semi-circular parasitic ring to enhance the bandwidth of the resonator over the desired frequency range (57–64 GHz). The parasitic semi-circular ring is designed to generate an additional resonance mode at 63.5 GHz to shift the resonator's lower 3 dB frequency from 59.2 to 58.2 GHz, as shown in Fig. 2. The SRR structure is fabricated on the top and bottom of the RT5880 substrate with relative permittivity of 2.2

and a thickness of 0.254 mm. To compute the S-parameters of proposed unit-cell, PEC and PMC boundary conditions were are assigned in the *xz* and *xy*-planes, respectively. Two wave-ports terminates the microstrip feedlines to excite the planar TEM wave.

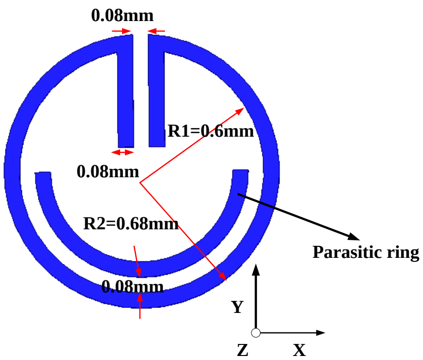

Fig. 1. The configuration of proposed split-ring resonator.

The proposed structures S-parameter response, shown in Fig. 2, exhibits a band-stop characteristic over the frequency range of 57–64 GHz, and the magnitude of the isolation is greater than 20 dB over 58.5–63.7 GHz.

III. MIMO ANTENNA

The DRA MIMO antenna design is based on reference [22]. The configuration of the proposed DRA structure with a relative permittivity of 10.2 is shown in Fig. 3. The antenna is constructed on a multi-layer substrate where the lower substrate is RT6010 with relative dielectric constant 10.2 and thickness of 0.254 mm. The feedlines are constructed on this substrate, which is necessary to excite the DRAs through a rectangular slot cut out of the upper substrate. The ground-plane is located on the bottom side of the lower substrate. The upper substrate is RT5880 with relative permittivity 2.2 and thickness of 0.254 mm. The DRs are mounted on top of this substrate immediately above the rectangular slot cut out in the substrate, as shown in Fig. 3.

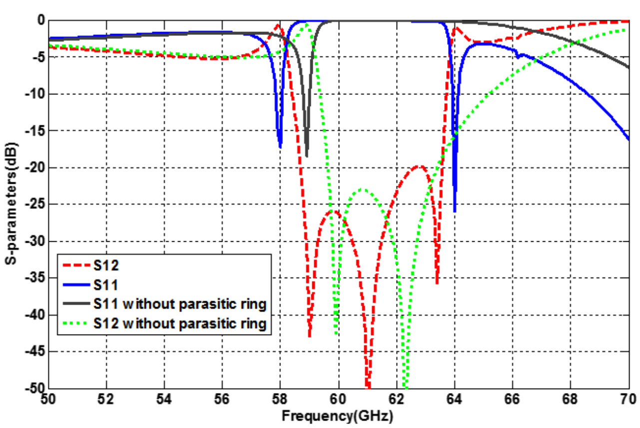

Fig. 2. The S-parameters of the modified shape of the split-ring resonator and the effect of the parasitic ring on the transmission coefficient response.

The array of 1×2 DRAs is arranged in the H-plane (*xz*) with a center-to-center distance of 2.5 mm corresponding to $\lambda_o/2$ at 60 GHz. The S-parameters response of DRA are shown in Fig. 4. The results indicate that the reflection coefficients of the antenna are better than -10 dB and the isolation is -18 dB over 57–64 GHz.

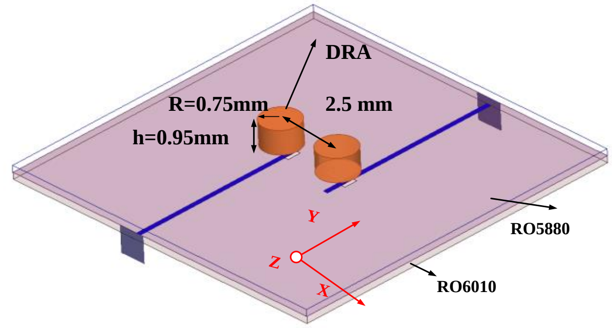

Fig. 3. The configuration of 1×2 DRAs arranged in the H-plane.

In order to reduce the electromagnetic interaction between the DRAs, a 1×7 array of the proposed SRR unit cell is implanted between the two Dielectric Resonators in the H-plane, as shown in Fig. 5. The S-parameters response of this structure in Fig. 4 show a considerable reduction in the mutual coupling. Isolation of -43 dB is obtained at 60 GHz, which corresponds to a reduction of 28 dB. The effect of locating a metal slab between DRAs is shown in Fig. 4. With the metal slab, the isolation is improved by only 5 dB at 60 GHz. The effect on the H-field with and without the metasurface is shown in Fig. 6. It is evident that the interaction is effectively curtailed with the location of the metasurface between the DRs in the *xz*-plane. The results confirm that the proposed array of SRR unit-cells has an effective band-stop property in the band 57–64 GHz.

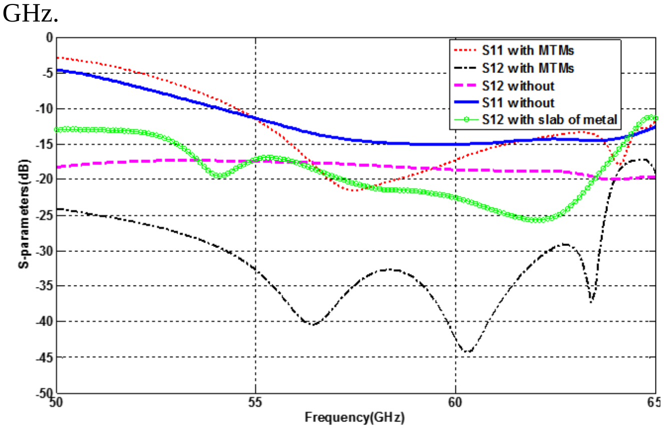

Fig. 4. The S11 and S12 response of the 1×2 DRAs antenna with and without metamaterial (MTM) unit cells along with a slab of metal for comparison.

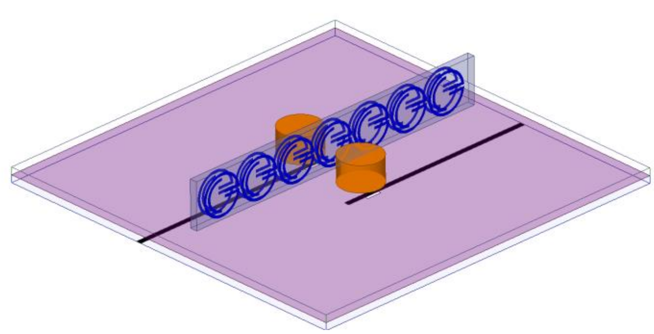

Fig. 5. Sketch of the configuration of 1×2 DRA with 1×7 metamaterial based SRR in the H-plane.

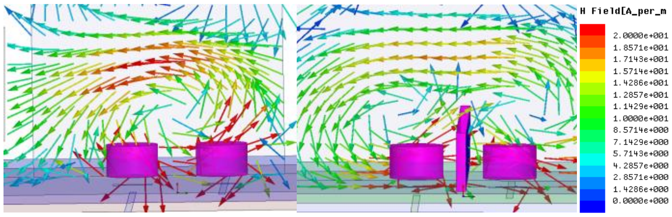

(a) (b)

Fig. 6. The H-field vector distribution in the H-plane, (a) without shielding, and (b) with a 1×7 array of metamaterial unit cells.

It is important to mention that the number of SRRs is selected through the parametric study as shown in Fig.7. It can be seen the best case is when the 7 SRRs are loaded between DRAs antenna.

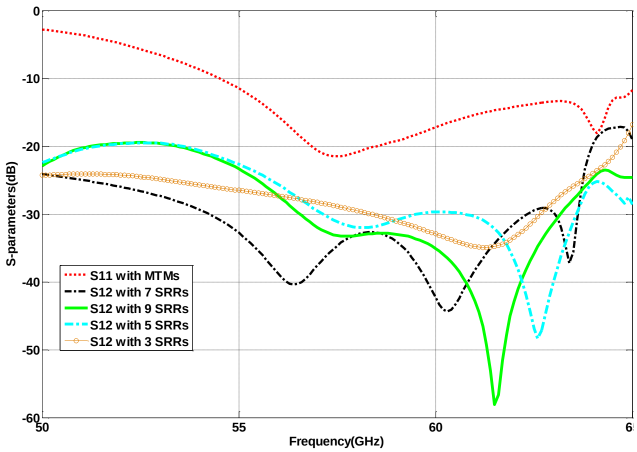

Fig. 7. The S12 response of the 1×2 DRAs antenna with a different number of SRRs.

IV. Experimental Results

The proposed 1×2 DRA that is integrated with a 1×7 array of SRR unit cells is fabricated, and its performance is measured. The photograph of the prototype antenna is shown in Fig. 8. The measured reflection coefficients of the antenna are shown in Fig. 9, which is better than -10 dB over 57–64 GHz. The measured isolation is -46.5 dB at 60.4 GHz and better than -30 dB over 59.3–64.8 GHz. A 1.85 mm end-launch connector (model no. 1893-03A-5) is used for the measurement.

In order to validate the simulation results, the radiation pattern of the proposed structure is measured when antenna port-1 is excited, and antenna port-2 is matched. The radiation pattern is measured in MI Technologies' compact range anechoic chamber. The transmitting antenna used is a horn. Spherical waves from the horn antenna were projected towards the reflector, which converted them to plane waves that were directed towards the receiver. The antenna under test is used as a receiving antenna and by rotating along its axis radiation patterns are measured in the E- and H-planes.

The normalized radiation pattern of the DRA antenna in the H-plane when integrated with the metasurface at different spot frequencies is shown in Fig. 10. It can be observed that the main peak direction is tilted by 35 degrees over the frequency range 58-64 GHz.

The measured E-plane and H-plane radiation pattern at 60 GHz with 1×7 SSR array are shown in Figs. 11 and 12, respectively. As can be observed the radiation pattern in the H-plane is tilted by 30 degrees with respect to the broadside radiation, which is attributed to the presence of the metasurface between the DRAs. In the E-plane (*yz*) the antenna radiates in the broadside direction.

(a) (b)

Fig. 8. (a) Photograph of 1×2 Dielectric Resonator Antenna with SRR arrays, (a) top view, and (b) feedline section.

The gain is measured using the comparison method where the power of the reference horn antenna and antenna under test are calculated separately. Then by considering the relative difference and knowing the gain of standard horn antenna the gain of DRA antenna is determined. The measured gain of DRA with a 1×7 array of metasurface is 7.9 dBi, which shows an improvement of 1.4 dB compared with the unloaded case. The radiation efficiency of the DRA with the metasurface is 91% at 60 GHz, which shows an improvement of 2% compared to the conventional DRA antenna.

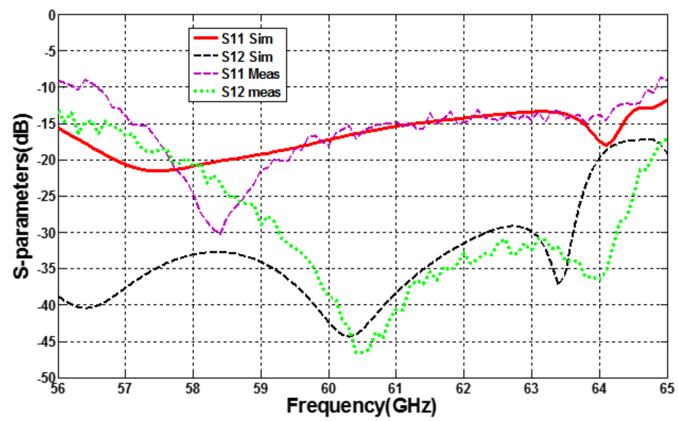

Fig. 9. The simulation and measured S-parameters of the 1×2 array of DRA with 1×7 array of SRR resonators.

V. Conclusion

An effective technique has been proposed that substantially reduces the mutual coupling between Dielectric Resonator Antennas at millimeter-waves for MIMO applications. This is achieved by incorporating a metasurface consisting of an array of split-ring resonator unit cells in the H-plane between the individual antennas. Measurements have shown that the isolation between antennas varies between -30 to -46.5 dB over 59.3–64.8 GHz, which constituted an improvement of 31.5 dB at 60.4 GHz.

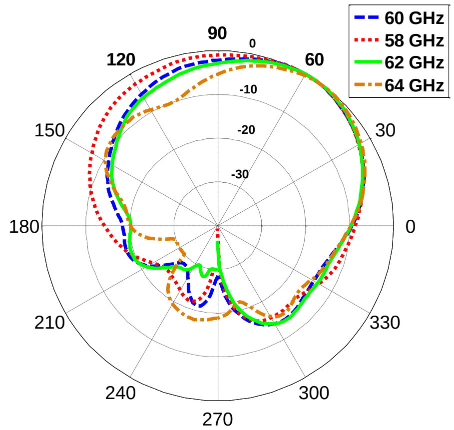

Fig. 10. The normalized radiation pattern of the DRA antenna with the metasurface consisting of 1×7 SSR array of unit cells at various frequencies in the H-plane (*xz*).

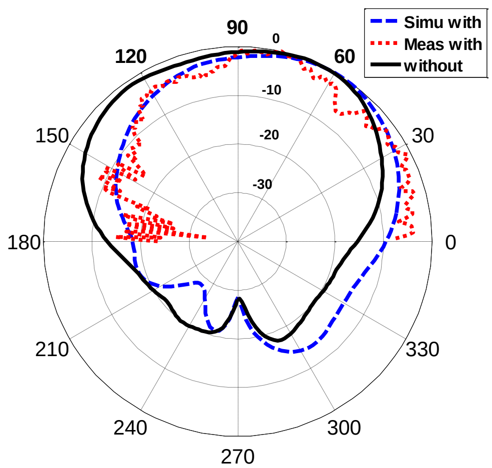

Fig. 11. The normalized radiation pattern of DRA antenna with and without metasurface consisting of 1×7 array of SRR unit-cells at 60 GHz in the H-plane (*xz*).

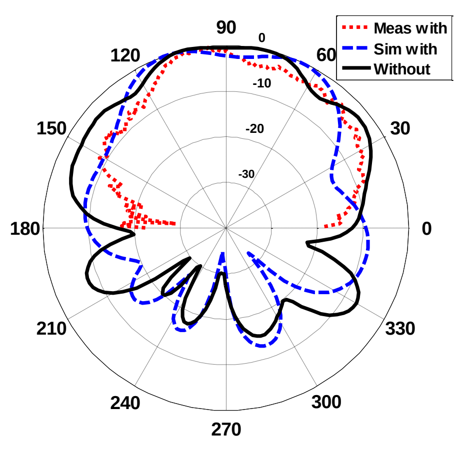

Fig. 12. The normalized simulated and measured radiation pattern of DRA antenna with and without metasurface consisting of a 1×7 array of SRR unit-cells at 60 GHz in the E-plane (yz).

REFERENCES

[1] Wireless Gigabit Alliance, Beaverton. www.wirelessgigabitalliance.org

[2] "Very High Throughput in 60 GHz," IEEE 802.11 TGad, Piscataway, NJ, 2010. www.ieee802.org/ 11/Reports/tgad_update.htm

[3] WirelessHD. www.wirelesshd.org/

[4] R. Karimian, H. Oraizi, S. Fakhte, and M. Farahani, "Novel F-Shaped Quad-Band Printed Slot Antenna for WLAN and WiMAX MIMO systems," *IEEE Antennas Wireless Propag. Lett*., vol. 12, pp. 405–408, 2013.

[5] Z. Y. Li, Z. W. Du, M. Takahashi, K. Saito, and K. Ito, "Reducing Mutual Coupling of MIMO Antennas with Parasitic Elements for Mobile Terminals," *IEEE Trans. Antennas Propag*., vol. 60, no. 2, pp. 473–481, Feb. 2012

[6] S. Assimonis, T. Yioultsis, and C. Antonopoulus, "Design and Optimization of Uniplanar EBG Structures for Low Profile Antenna Applications and Mutual Coupling Reduction," *IEEE Trans. Antennas Propag*., vol. 60, no. 10, pp. 4944–4949, 2012.

[7] A. Lamminen, A. Vimpari, and J. Saily, "UC-EBG on LTCC for 60-GHz Frequency Band Antenna Applications," *IEEE Trans. Antennas Propag.*, vol. 57, pp. 2904–2912, Oct. 2009.

[8] S. Assimonis, T. Yioultsis, and C. Antonopoulus, "Mutual Coupling Reduction in Waveguide Slot-Array Antennas Using Electromagnetic Bandgap (EBG) Structures," *IEEE Antennas and Propag. Mag*., vol. 56, no. 3, pp. 68–79, 2014.

[9] E. R. Iglesias, O. Q. Teruel, and L. I. Sanchez, "Mutual coupling reduction in patch antenna arrays by using a planar EBG structure and a multilayer dielectric substrate," *IEEE Trans. Antennas Propag*., vol. 56, no. 6, pp. 1648–1655, Jun. 2008.

[10] Quevedo-Teruel, O.; Inclan-Sanchez, L.; Rajo-Iglesias, E. "Soft Surfaces for Reducing Mutual Coupling Between Loaded PIFA Antennas", *IEEE Antennas Wireless Propag. Lett*., vol. 9, pp. 91–94, 2010.

[11] Attia, H.; Sorkherizi, M.S.; Kishk, A.A. "60 GHz PRGW slot antenna array with small separation and low mutual coupling", *Millimeter Waves (GSMM), Global Symposium*,2015,pp. 1 - 3

[12] G. Exposito-Dominguez, J.M. Fernandez-Gonzalez, P. Padilla, M. Sierra-Castaner, "Mutual Coupling Reduction Using EBG in Steering Antennas," *IEEE Antennas and Wireless Propagation Letters,* Vol. 11, pp. 1265–1268, 2012.

[13] D.A. Ketzaki, and T.V. Yioultsis, "Metamaterial-Based Design of Planar Compact MIMO Monopoles," *IEEE Trans. Antennas Propagat*., Vol. 61, no. 5, pp. 2758–2766, May 2013.

[14] H.X. Xu, G.M. Wang, and M.Q. Qi, "Hilbert-Shaped Magnetic Waveguided Metamaterials for Electromagnetic Coupling Reduction of Microstrip Antenna Array," *IEEE Trans. Magn*., vol. 49, no. 4, pp. 1526–1529, 2013.

[15] S. Zhang, and G.F. Pedersen, "Mutual Coupling Reduction for UWB MIMO Antennas with a Wideband Neutralization Line," *IEEE Antennas and wireless propagation letters*. To be published, 2015.

[16] M. Gulam, N. Alsath, M. Kanagasabai, and B. Balasubramanian, "Implementation of Slotted Meander-Line Resonators for Isolation Enhancement in Microstrip Patch Antenna Arrays," *IEEE Antennas and Wireless Propagation Letters*, vol. 12, 12 March 2013, pp. 15–18.

[17] G. Zhai, Z.N. Chen, and X.Qing, "Enhanced Isolation of a Closely Spaced Four-Element MIMO Antenna System using Metamaterial Mushroom," *IEEE Trans. Antennas Propag*., vol. 63, no. 8, pp. 3362–3370, Feb. 2015

[18] M.S. Sharawi, M.U. Khan, A.B. Numan, and D.N. Aloi, "A CSRR Loaded MIMO Antenna System for ISM Band Operation," *IEEE Trans. Antennas Propag*., vol. 61, no. 8, pp. 4265–4274, Aug. 2013

[19] S. Farsi, H. Aliakbarian, D. Schreurs, and B. Nauwelaers, "Mutual Coupling Reduction Between Planar Antennas By Using a Simple Microstrip U-Section," *IEEE Antennas Wireless Propag. Lett.*, vol. 11, pp. 1501–1503, Dec. 2012.

[20] M.J. Al-Hasan, T.A. Denidni, A.R. Sebak, "Millimeter-Wave EBG-Based Aperture-Coupled Dielectric Resonator Antenna," *IEEE Trans. Antennas Propagat*., vol.61, no.8, pp.4354,4357, Aug. 2013

[21] R. J. Dorris, R. T. Long, S. A. Long, M. A. Khayat, and Jeffety T. Williams, " Mutual coupling between cylindrical probe-fed dielectric resonator antennas," *IEEE Antennas and Wireless Propagation Letters*, vol. 1, no. 1, pp. 8-9,2002

[22] A. Hagras, T.A. Denidni, M. Nedil, Y. Coulibaly, "Low-Mutual Coupling Antenna Array for Millimeter Wave MIMO Applications," *IEEE Antennas and Propagation Society International Symposium (APS/URSI)*, 8-14 July 2012, pp. 1–2.